

# Electron microscopic heteroduplex analysis of "killer" double-stranded RNA species from yeast\*

(RNA-RNA hybridization/defective interfering virus)

HOWARD M. FRIED<sup>†</sup> AND GERALD R. FINK<sup>‡</sup>

Section of Botany, Genetics and Development, Cornell University, Ithaca, New York 14853

Communicated by Adrian M. Srb, June 21, 1978

**ABSTRACT** Wild-type and mutant double-stranded RNA (dsRNA) species from the yeast *Saccharomyces cerevisiae* were studied by electron microscopic heteroduplex mapping to determine the sequence relationships among the different RNA molecules. Three mutant dsRNAs, 1.5, 1.4, and 0.73 kilobase, were found to be derived by the same internal deletion of the wild-type (1.83 kilobases) molecule. This deletion includes a segment of about 200 base pairs that was estimated to be nearly 100% A + U. In addition, the sequences of the two larger mutant RNA species are tandem, direct duplications. One of the duplicated molecules appears to have a second internal deletion that occurred after the duplication. The mutant dsRNAs are functionally similar to the defective interfering virus particles of animal viruses—all of the mutant species prevent the propagation of the wild-type dsRNA when both are present in the same cell. The four dsRNAs share the same sequences at their termini, a finding that may suggest that these sequences are important for the replication of the dsRNAs.

Viruses and virus-like particles containing double-stranded RNA (dsRNA) are common to many species of fungi (1). Killer strains of the yeast *Saccharomyces cerevisiae* possess viral particles with two separately encapsidated dsRNA species: large (L),  $2.5 \times 10^6$  daltons; and medium (M),  $1.18 \times 10^6$  daltons (see refs. 2 and 3 for recent reviews). These strains excrete a toxic protein that kills sensitive strains but not killer strains. The M-dsRNA was believed to produce toxin and immunity to toxin because (i) the non-Mendelian segregation of these two killer traits is paralleled by cytoplasmic transmission of the dsRNA, and (ii) strains with an alteration in either toxin production or immunity either lack the M-dsRNA or have an altered form of it (4, 5). Recently, *in vitro* translation experiments have proved that M encodes the killer toxin (J. Hopper, personal communication). Denatured M-dsRNA directed the synthesis of a protein that, although larger than killer toxin, crossreacted with antiserum to toxin and contained all of the tryptic peptides of toxin produced *in vivo*. In similar *in vitro* experiments, the L-dsRNA directed the synthesis of the major capsid protein of the virus-like particles (6).

Nonkiller mutants have been isolated that lack the M-dsRNA but have smaller (S) dsRNA species (7). When these mutants are mated to a killer strain the S-dsRNAs prevent or "suppress" the propagation of the M-dsRNA in the resulting diploids. With continued growth, the diploid cells rapidly become nonkillers and the M-dsRNA can no longer be detected. These suppressive S-dsRNAs therefore, are analogous to defective interfering virus particles, the subgenomic nucleic acid species of animal viruses that limit the replication of the standard virus during co-infection (8).

This report describes electron microscopic heteroduplex mapping experiments between the M- and S-dsRNAs. The

heteroduplexes studied show that the S-dsRNAs arose by deletions of M-dsRNA sequences. The various S-dsRNAs are also related to each other by sequence reiteration or further deletion. One aspect is common to all the suppressive S-dsRNAs—namely, the sequences at both ends of M-dsRNAs are retained as termini in the S-dsRNAs.

## MATERIALS AND METHODS

**Yeast Strains.** The killer (A8209B) and suppressive nonkiller (T132B NK 17, 19, and 20) strains have been described (7). The suppressive strains were derived directly from the same parent strain, T132B, a derivative of A8209B that has the property of segregating killers and suppressive nonkillers.

**Chemicals.** Formamide (Matheson, Coleman, and Bell) was purified twice by recrystallization at 0° (9).

**Preparation of dsRNA.** dsRNA was prepared from unbroken cells; this method reduced contamination by DNA and ribosomal RNA (4). Cells were washed with 50 mM Na<sub>2</sub>EDTA (pH 7.0), incubated for 15 min in 50 mM Tris-H<sub>2</sub>SO<sub>4</sub> (pH 9.3) containing 2.5% 2-mercaptoethanol, and then stirred for 1 hr at room temperature with 0.1 M NaCl/10 mM Tris-HCl, pH 7.5/10 mM Na<sub>2</sub>EDTA/0.2% sodium dodecyl sulfate and an equal volume of redistilled phenol. Nucleic acid in the aqueous phase was recovered by ethanol precipitation, dissolved in 2.0 M LiCl/0.15 M NaCl/0.015 M Na<sub>3</sub> citrate and incubated at least 8 hr at 4°. The resulting LiCl precipitate was removed by centrifugation and the nucleic acid in the supernatant was recovered with ethanol and electrophoresed under nondenaturing conditions on a 1.5% agarose slab gel containing 1 µg of ethidium bromide per ml (10). To recover the dsRNA, the gel bands were visualized with shortwave UV illumination, cut out, homogenized, and extracted with 0.3 M NaCl/50 mM Tris-HCl, pH 7.5/5 mM Na<sub>2</sub>EDTA and an equal volume of phenol (2 hr, 37°). The RNA was precipitated from the aqueous phase with 2 vol of ethanol at -20° and recovered by centrifugation (175,000 × g, 90 min). The RNA was dissolved in 100–200 µl of 0.1 M Tris-HCl, pH 7.0/10 mM Na<sub>2</sub>EDTA and dialyzed extensively against the same buffer.

**Electron Microscopy.** Native molecules were mounted for electron microscopy, according to the isodenaturing spreading procedure of Davis *et al.* (11), from a 50-µl hyperphase containing 60% formamide, 30 mM Tris-HCl (pH 8.3), 3 mM Na<sub>3</sub>EDTA, 40 µg of cytochrome *c* per ml, and 0.2–0.5 µg of RNA per ml on to a hypophase of 30% formamide/3 mM Tris-HCl/0.3 mM Na<sub>3</sub>EDTA. The cation concentration of the hyperphase was about 20 mM.

For hybridization experiments, RNA was mixed in 25 µl of

The publication costs of this article were defrayed in part by page charge payment. This article must therefore be hereby marked "advertisement" in accordance with 18 U. S. C. §1734 solely to indicate this fact.

Abbreviations: dsRNA, double-stranded RNA; L, large; M, medium; S, small; kb, kilobases;  $t_m$ , melting temperature.

\* This paper is dedicated to the memory of Dr. Alvin Nason.

<sup>†</sup> Present address: Department of Biochemistry, Albert Einstein College of Medicine, Bronx, NY 10461.

<sup>‡</sup> To whom reprint requests should be addressed.

the same hyperphase (without cytochrome *c*) at 1–2  $\mu\text{g}/\text{ml}$ , either with or without a second RNA species at the same concentration. The RNA was denatured by heating at 70° for 1 min; after the cation concentration was increased to 0.1 M with 1  $\mu\text{l}$  of 2.6 M Tris-HCl, pH 8.3/0.26 M Na<sub>3</sub>EDTA, hybridization was begun by incubation at 40°. A 10- $\mu\text{l}$  sample was taken before incubation and after 15 or 30 min at 40°, diluted with 40  $\mu\text{l}$  of 60% formamide, and spread.

Contour length measurements of molecules were made with an electronic planimeter (Numonics Corp.) from films exposed at a magnification of  $\times 12,500$  and enlarged 10-fold in a photographic enlarger. The DNA plasmid PSC101 (12) was added to all samples (0.1  $\mu\text{g}/\text{ml}$ ) before spreading to serve as an internal length standard [9.2 kilobases (kb)]. Lengths of dsRNA, expressed as fractional lengths of PSC101 from the same film, were converted to molecular weight by multiplying by the size of PSC101 and then by 1.18, the ratio of the mass/unit length of dsRNA to dsDNA (13). The molecular weights were corrected further by multiplying by 0.89 because we found that, relative to the plasmid DNA, the dsRNA was 11% longer in the formamide spreads than in high ionic strength (0.5 M) aqueous spreads.

A conversion factor relating the length of single-stranded RNA to its molecular weight was obtained from measurements of denatured M-dsRNA. The number average length ( $\pm$ SD) of 156 single-stranded molecules was  $0.582 \pm 0.033 \mu\text{m}$  (assuming a length of 3  $\mu\text{m}$  for PSC101), which yields a factor of  $1.10 \times 10^6$  daltons/ $\mu\text{m}$  (the size of one strand of M is  $0.59 \times 10^6$  daltons; see below). This value agrees with the mass per unit length reported for 18S and formaldehyde-treated 28S ribosomal RNAs in solutions of similar denaturing properties (14). Under our experimental conditions, no secondary structure was observed in the denatured RNA.

## RESULTS

The dsRNA species of the killer and suppressive nonkiller strains were separated on 1.5% agarose slab gels (Fig. 1). All of the strains contained the L-dsRNA. The suppressive strains T132B NK 17, 19, and 20 lacked the M-dsRNA of the killer, but they had the smaller RNA species designated S1, S3, and S4, respectively. The sizes (mean  $\pm$  SD) of the dsRNAs, determined under the conditions of electron microscopy used, are  $1.83 \pm 0.05$  ( $n = 173$ ),  $1.50 \pm 0.05$  ( $n = 194$ ),  $1.40 \pm 0.06$  ( $n = 228$ ), and  $0.73 \pm 0.04$  kb ( $n = 191$ ) for M, S1, S4, and S3. These sizes agree with the molecular weights determined previously under different conditions of electron microscopy (7). In the presence of the denaturing agent methylmercuric hydroxide, electrophoresis of the dsRNAs resulted in sharp bands with mobilities equivalent to half their molecular weights, a result that indicated that the RNAs were free of hidden single-stranded breaks and proved that they did not exist in a hairpin structure (data not shown).

**Electron Microscopy of Native dsRNA Molecules.** To observe unpaired segments in heteroduplexes the conditions of electron microscopy used were chosen because they were expected to cause sufficient extension of single-stranded RNA. With these conditions, we observed routinely a large bubble ( $0.20 \pm 0.04$  kb,  $n = 173$ ) in the center of the M-dsRNA molecule (Fig. 2A). Usually, 50–70% of the molecules had this bubble and its position was the same in each molecule. The bubble, however, was never observed in any of the S-dsRNA species, a fact that was later useful in describing the sequence relationships among the RNA species (see below). Increasing the cation concentration of the hyperphase from 20 mM to 80 mM

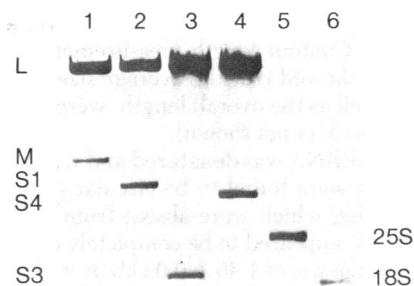


FIG. 1. Agarose slab gel electrophoresis of yeast dsRNAs. Extracts of killer (A8209 B) and suppressive nonkiller (T132B NK 17, T132B NK 19, and T132B NK 20) strains are shown in lanes 1–4, respectively. The dsRNA species are designated at the left. The extracts were treated with DNase I (40 units/ml) to eliminate DNA which otherwise forms a sharp band above the band of L-dsRNA. Lanes 5 and 6 contain 25S and 18S ribosomal RNA, purified by agarose gel electrophoresis of extracts prepared according to J. Warner (personal communication).

decreased the frequency of the bubble to about 25% of the molecules, suggesting that the bubble is the result of partial denaturation of the M-dsRNA. The nucleotide base composition of this denatured segment was estimated from the fact that the conditions of the hyperphase were found (by spectrophotometry) to lower the overall melting temperature ( $t_m$ ) of the dsRNAs by 44° (data not shown). Therefore, the bubble had a standard aqueous (0.2 M cation)  $t_m$  of about 67° which implies a base composition of nearly 100% A + U (15).

**Electron Microscopy of Denatured and Reannealed dsRNA Molecules.** We determined a hybridization protocol for the dsRNAs with the M-dsRNA and various combinations of temperature, time, and ionic strength. Several criteria were used to assess denaturation and renaturation. Complete strand separation was monitored by the total absence of molecules containing a bubble. The mass/unit length measured for the denatured molecules was consistent with their being intact single strands. When M-dsRNA was reannealed, only linear

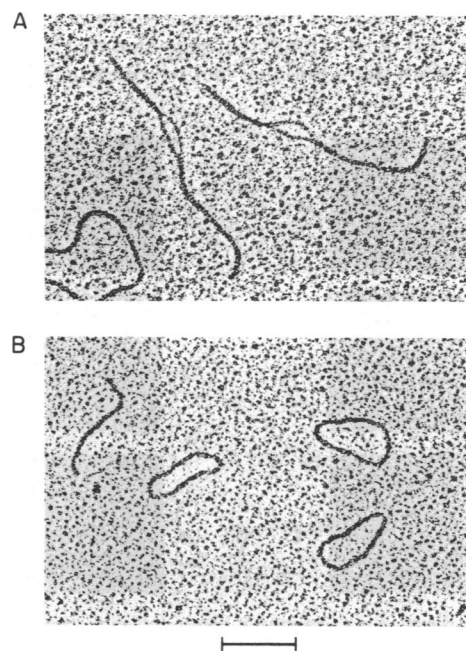


FIG. 2. Electron micrographs of native M-dsRNA and reannealed S1-dsRNA. (A) Native M-dsRNA in 60% formamide/20 mM cation. (B) Reannealed S1 in 60% formamide/20 mM cation. Scale represents 0.5 kb (double-stranded) or 0.44 kb (single-stranded).

<sup>§</sup>  $n$  in parentheses refers to the number of molecules measured.

molecules were observed, many of which now had the denaturation bubble. Contour length measurements of 135 renatured molecules showed that the average size and position of the bubble, as well as the overall length, were the same as for native molecules (data not shown).

When the S1-dsRNA was denatured and reannealed, many of the molecules were found to be circular (Fig. 2B). These circular molecules, which were absent from preparations of native S1-dsRNA, appeared to be completely double-stranded and had an average size of  $1.46 \pm 0.06$  kb ( $n = 157$ ), essentially equal to that of native S1. Circular molecules were not seen in hybridization of S3 with M (see below), so we concluded that S3 does not circularize upon reannealing.

To determine the sequence relationships among the M-, S1-, and S3-dsRNAs, the RNAs were hybridized to each other. When M was hybridized to S1, a number of structures were observed consisting of double-stranded segments and single-stranded "loops" and "tails". The example in Fig. 3A contains two single-stranded segments; it is not a molecule with a large denaturation bubble because the two single-stranded segments have different sizes ( $1.14 \pm 0.11$  and  $0.82 \pm 0.08$  kb,  $n = 98$ ). The examples in Fig. 3B and C appear similar to each other but they are in fact different. Thirty-six examples like Fig. 3B and 23 examples like Fig. 3C were found to have the same size single-stranded tail ( $0.70 \pm 0.08$  kb), the same size loop ( $1.18 \pm 0.09$  kb), and the same two short duplex segments ( $0.50 \pm 0.04$  and  $0.22 \pm 0.03$  kb). However, the tail on the form in Fig. 3B adjoins the longer duplex segment whereas the tail on that in Fig. 3C adjoins the shorter. The example in Fig. 3D also has the same loop and tail but in this case the tail adjoins a much larger duplex ( $1.23 \pm 0.09$  kb,  $n = 5$ ). The example in Fig. 3E contains two loops separated by a  $0.79 \pm 0.07$  kb duplex, as well as the two smaller duplex segments. All of these structures were observed in every experiment involving M- and S1-dsRNA; they are hybrid molecules because they were observed only if the two species were mixed. Finally, when M was hybridized to S3, only one type of heteroduplex was found (Fig. 3F).

These results in conjunction with data communicated to us by J. Bruenn were used to devise a model to describe the sequence relationships of the dsRNAs. A critical piece of information was that the RNA fingerprint of S1-dsRNA was exactly the same as that of S3, a result that suggested that S1 is a dimer of S3 (16). With this additional fact we constructed a model,

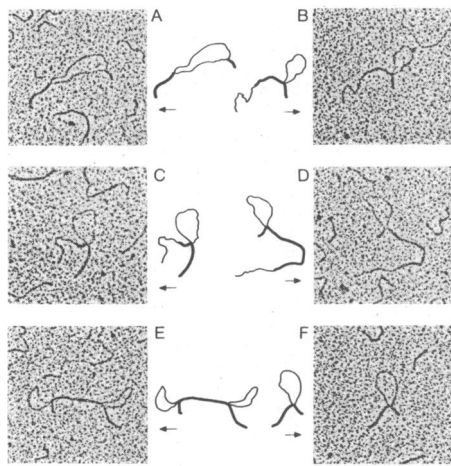


FIG. 3. Electron micrographs of heteroduplex molecules obtained in hybridizations of the M-dsRNA with either S1- or S3-dsRNAs. (A-E) M-S1 heteroduplexes. (F) M-S3 heteroduplex. The drawings in the center are interpretations of the molecules, showing single- and double-stranded segments. Scale represents 0.5 kb (double-stranded) or 0.44 kb (single-stranded).

outlined in Fig. 4A, of the sequence relationships of the M-, S1-, and S3-dsRNAs. The S3-dsRNA (ABC I) was assumed to be derived from M-dsRNA (ABCDEF GHI) by an internal deletion of 60% (the difference in size between M and S3) which covers the denaturation bubble. Hybridization of M with S3 then yields heteroduplex VIII (Fig. 3F). The S1-dsRNA was postulated to be a tandem, direct duplication of S3. When denatured S1 is reannealed it is able to form circular structures with a contour length identical with that of native S1 (I); furthermore, by hybridizing to M, S1 generates the three primary heteroduplexes II, III, IV shown in Fig. 3 A-C. Two of these hybrids have single-stranded tails that are free to pair with an additional strand of either M or S1 to give molecules VI and VII of Fig. 3 E and D, respectively.

The interpretation given in Fig. 4A was supported by the contour length measurements (Table 1) of all the various segments of each heteroduplex. These data showed that a given single-stranded or double-stranded segment had the same av-

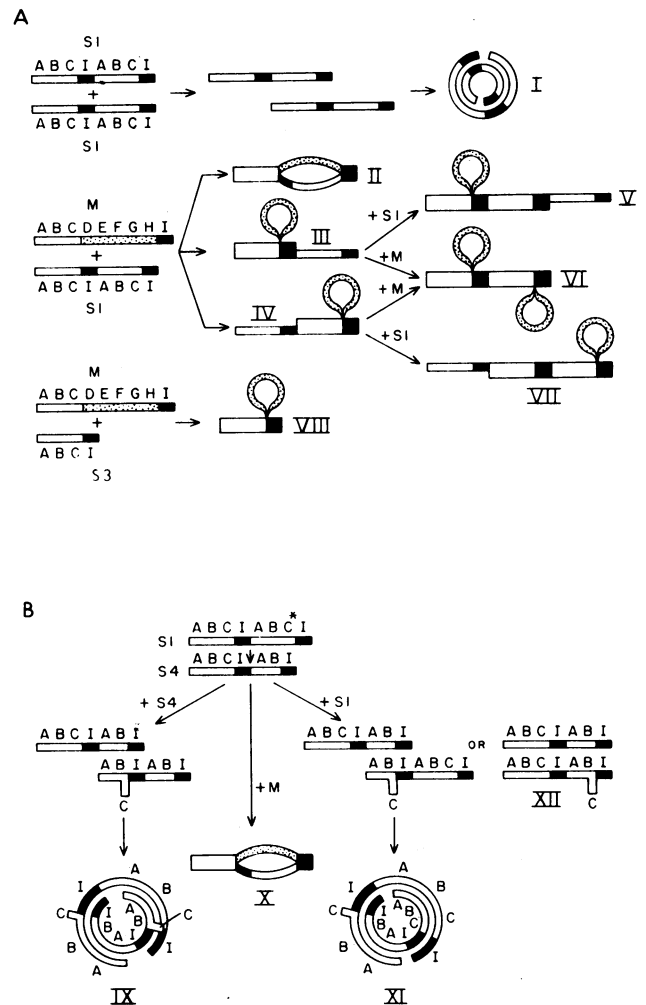


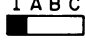

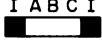



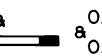


FIG. 4. Models describing sequence relationships among the M- and S-dsRNA species. Thin rectangular blocks represent single-stranded (unpaired) segments and thick blocks represent double-stranded (paired) segments. Each letter above the blocks represents a segment of about 200 nucleotides or nucleotide pairs. (A Top) Pairing of complementary strands of S1-dsRNA results in circular double-stranded molecules. (A Middle and Bottom) Pairing of single strands of M and S1 or S3 produces the heteroduplexes described in Results. (B Left) Pairing of complementary strands of S4 results in circular homoduplexes with two unpaired but complementary segments ("C"). (B Right) Pairing of single strands of S4 and S1 produces circular or linear heteroduplexes with one unpaired segment. Asterisk above S1 indicates hypothetical deletion to give S4.

Table 1. Contour length measurement data for segments of hybrid dsRNA molecules

Segment	$\bar{L}_N \pm SD$ (kilobases)	Number of molecules
<b>I. Double-stranded</b>		
	$0.50 \pm 0.04$	280
	$0.22 \pm 0.03$	291
	$0.79 \pm 0.07$	11
	$1.23 \pm 0.09$	5
	ND	ND
<b>II. Single-stranded</b>		
	$1.14 \pm 0.11$	98
	$1.18 \pm 0.09$	86
	$0.82 \pm 0.08$	98
	$0.70 \pm 0.08$	64

$\bar{L}_N \pm SD$  = number average length  $\pm$  SD; ND = not determined.

erage size in each type of structure in which it occurred. Moreover, the combined sizes of the various segments of a given structure equaled the total size of the two (or three) molecules that were paired to produce the hybrid. For example, the two double-stranded ends of the M-S1 heteroduplex in Fig. 3A (i.e., ABC and I) averaged 0.50 and 0.22 kb. One of the single-stranded segments of this structure was 1.14 kb; the total, 1.86 kb, is the size of native M-dsRNA. The other single-stranded segment was 0.82 kb and gave a total of 1.54 kb, which agrees closely with the size of native S1-dsRNA.

The sequence arrangement of the S4-dsRNA was investigated in a similar fashion. When reannealed alone, S4 was found to form circular structures also but these circles differed from those produced by S1 because they contained a short linear tail that appeared to be double-stranded (Fig. 5 A and B). Nevertheless, in hybridization experiments the S4-dsRNA combined with M to give the same series of heteroduplex structures as was observed for a mixture of S1 and M. Length measurements of heteroduplex X (shown in Fig. 5C) showed that the terminal double-stranded ends of this hybrid ( $0.51 \pm 0.03$  and  $0.23 \pm 0.03$  kb,  $n = 55$ ) were the same sizes as their counterparts in the analogous M-S1 hybrid (i.e., II). Also, the single-stranded segments of this structure ( $1.08 \pm 0.10$  and  $0.68 \pm 0.08$  kb) corresponded to the sizes of the remainder of the M and S4 molecules. These results, therefore, suggested that S4 is a tandem duplication like S1 and that S4 is also related to M by at least the same deletion as the one that produced S1 and S3. Yet, the observations did not explain the difference between the S1 and S4 circular molecules that result from reannealing of these species alone.

A possible explanation for the difference between S1 and S4 is outlined in Fig. 4B. The S4-dsRNA, which is 7% smaller than S1, is assumed to be derived from S1 by a small deletion. This deletion may be anywhere in S1 except within the terminal sequences which S1 shares with M. As a result of the deletion, when the complementary strands of S4 pair to form a circle, two short, unpaired segments will be produced (IX). An example

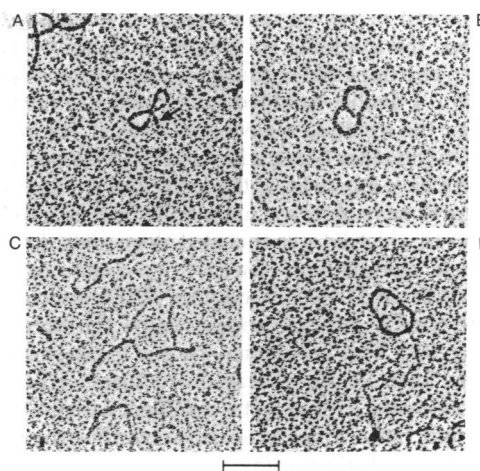


FIG. 5. Electron micrographs of molecules formed in hybridization with S4-dsRNA. (A and B) Circular S4 homoduplex (arrow in A indicates double-stranded tail). (C) M-S4 heteroduplex. (D) Circular S4 homoduplex; the two short protrusions are believed to be unpaired segments that ordinarily anneal to form the double-stranded tail. Scale represents 0.5 kb (double-stranded) or 0.44 kb (single-stranded).

of such a structure is the molecule shown in Fig. 5D. Because these unpaired segments have complementary nucleotide sequences, they can also anneal to each other, thereby forming circular molecules with a double-stranded tail. Actually, only two or four examples of the molecule in Fig. 5D were found among several hundred circular molecules; yet, this infrequent observation is not surprising because the postulated unpaired segments are closely apposed and so should almost always anneal to each other.

To try to confirm the sequence arrangement of S4-dsRNA, we examined hybridizations between S4 and S1. As shown in Fig. 4B, an S1-S4 heteroduplex is expected to be either a circular (XI) or a linear structure (XII) with one unpaired segment. Two molecules that appear to be examples of structure XI are illustrated in Fig. 6. These structures resemble the expected S1-S4 hybrid, although it was often difficult to distinguish them from the circular S4 homoduplexes which have a tail (such as the one in Fig. 5B), even though the short unpaired segment of the S1-S4 heteroduplex should be single-stranded

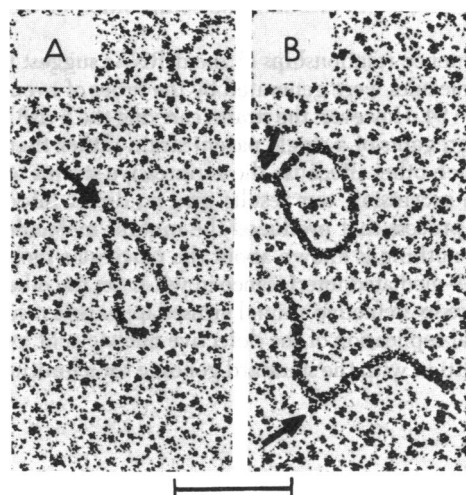


FIG. 6. Examples of possible heteroduplexes from S1-S4 hybridization experiments. The three molecules have a short extending segment (indicated by arrows) that is thought to result from a loop of unpaired S1-RNA. Scale represents 0.5 kb (double-stranded).

whereas the tail of the S4 homoduplex is double-stranded. Nevertheless, the examples shown are probably hybrids because, when two unpaired segments in an S4 homoduplex anneal to form a double-stranded tail, topological constraints should cause the resulting molecule to form a "figure 8" (see Fig. 5A). On the other hand, a heteroduplex between S1 and S4 should not have any twist, as the molecules in Fig. 6. In fact, fewer figure 8s were observed in S1-S4 hybridizations than in experiments in which S4 was annealed alone (data not shown). Despite these observations, however, we could not identify positively the linear S1-S4 heteroduplex (XII) predicted by the model (one possible example appears below the circular molecule in Fig. 6B). This failure may be due to the small size of the expected loop. No other unusual structures were observed in these experiments, a result that is consistent with the proposed interpretations, but a firmer conclusion regarding the structure of S4 should await further study.

### DISCUSSION

The present electron microscopic study has revealed many aspects of the structure of the yeast dsRNAs. Within the resolution of the methods, the three suppressive S-dsRNAs are all derived from the wild-type M-dsRNA by the same internal deletion. Two of the S-dsRNAs contain a tandem duplication and one of the duplicated molecules has a further deletion. These conclusions, which we think are the simplest explanation of the heteroduplexes, are based on the contour length measurement data given above and the reported RNA fingerprint analysis (16). The difficulty encountered in distinguishing S1-S4 heteroduplexes could probably be overcome with additional techniques. Because the S4- and S1-dsRNAs differ in size by about 100 base pairs, the small loop in an S4-S1 heteroduplex (assuming S4 is a simple deletion of S1) might be resolved better with the aid of T4 or *Escherichia coli* single-stranded DNA binding proteins.

The M-dsRNA contains a 200-base pair sequence that was estimated to be nearly 100% A + U. Large tracts of A or U have not been found by RNA fingerprint analysis of M (16). However, the denaturing effect of formamide is greater on dA-dT homopolymers than on average sequences (9) and it is likely that a similar effect would apply to rA-rU. It is thus possible that the 200-base pair segment contains some G-C base pairs because the effect of formamide on the  $t_m$  of the *entire* M-dsRNA molecule was used to estimate the composition of the 0.2-kb segment.

The sequence relationships of the dsRNAs suggest that the mutant molecules were generated by the series of events M → S3 → S1 → S4. However, the strains carrying the S-dsRNAs are mitotic segregants of a single parent strain rather than segregants of each other. Because the suppressive strains were not derived in succession, our results give no direct information about the process that produced the mutant molecules. Furthermore, nothing is known about the particular mechanism of S-dsRNA-mediated interference in yeast. On the other hand, interference by defective animal viruses appears to result from preferential replication of the defective nucleic acid, probably by competition with the standard genome for a limiting repli-

cation factor. Earlier studies of the defective genomes of some single-stranded RNA viruses indicated that mutant molecules are derived by internal deletions of the standard virus (17-20). These results were consistent with the expectation that the defective molecules retain the origins of replication in order to compete with the standard virus.

Recent studies, however, reveal that the defective molecules of some negative-strand RNA viruses are derived from the 5' end of the standard genome whereas the 3' portion is not retained (21, 22). It appears that, during replication along the plus-strand template, a nascent minus-strand forms a hairpin loop upon itself and the replicase enzyme finishes its synthesis by using the 5' end of the nascent strand as template. Nevertheless, it seems likely that the sequences conserved in the defective molecules are necessary for replication. The sequences present at the termini of the yeast M-dsRNA are retained as *termini* in all three suppressive dsRNAs we studied, even though two of the molecules were duplicated and one acquired a further deletion. Conservation of these sequences may therefore imply that the S-dsRNAs interfere with the propagation of the M-dsRNA at the level of replication.

We are indebted to Drs. Louise Chow and Tom Broker for teaching us the art of electron microscopy. This work was supported by Grant PCM 76-11667 from the National Science Foundation. H.M.F. was a predoctoral trainee under Grant 5T 01 GM 00824 from the National Institutes of Health.

- Lemke, P. A. (1976) *Annu. Rev. Microbiology* **30**, 105-144.
- Wickner, R. B. (1976) *Bacteriol. Rev.* **40**, 757-773.
- Pietras, D. F. & Bruenn, J. A. (1976) *Int. J. Biochem.* **7**, 173-179.
- Fried, H. (1978) Dissertation (Cornell University, Ithaca, NY).
- Vodkin, M., Katterman, F. & Fink, G. (1974) *J. Bacteriol.* **117**, 681-686.
- Hopper, J. E., Bostian, K. A., Rowe, L. B. & Tipper, D. I. (1978) *J. Biol. Chem.* **252**, 9010-9017.
- Sweeney, T. K., Tate, A. & Fink, G. (1976) *Genetics* **84**, 27-42.
- Huang, A. S. (1973) *Annu. Rev. Microbiology* **27**, 101-117.
- Casey, J. & Davidson, N. (1977) *Nucleic Acids Res.* **4**, 1539-1552.
- Sugden, B., DeTroy, B., Roberts, R. J. & Sambrook, J. (1975) *Anal. Biochem.* **68**, 36-46.
- Davis, R. W., Simon, M. & Davidson, N. (1971) in *Methods in Enzymol.* **21**, 413-428.
- Wensink, P. C., Finnegan, D. J., Donelson, J. E. & Hogness, D. S. (1974) *Cell* **3**, 315-325.
- Langridge, R. & Gomas, P. J. (1963) *Science* **141**, 694-698.
- Wellauer, P. K. & Dawid, I. B. (1974) *J. Mol. Biol.* **89**, 379-395.
- Kallenbach, N. R. (1968) *J. Mol. Biol.* **37**, 445-466.
- Bruenn, J. A. (1978) *J. Virol.* **26**, 762-772.
- Kennedy, S. I. T. (1976) *J. Mol. Biol.* **108**, 491-511.
- Johnson, L. D. & Lazzarini, R. A. (1977) *Virology* **71**, 863-866.
- Keene, J. D., Rosenberg, M. & Lazzarini, R. A. (1977) *Proc. Natl. Acad. Sci. USA* **74**, 1383-1357.
- Guild, G. M. & Stollar, V. (1977) *Virology* **77**, 175-188.
- Leppert, M., Kort, L. & Kolakofsky, D. (1977) *Cell* **12**, 539-552.
- Huang, A. S. (1977) *Bacteriol. Rev.* **41**, 811-821.